Key Points:
- We study future competition between irrigation and other water uses with a detailed integrated model of economic and hydrological processes
- We find that even substantial water use efficiency improvements have little impact on water deficits (demand minus allocated water volume)
- Local allocation rules have a large effect on water deficits, whereas a basin-level strategy of limiting irrigation has less effect

Supporting Information:
- Supporting Information S1
- Data Set S1

Correspondence to:
D. L. Bijl,
dlbijl@gmail.com

A Global Analysis of Future Water Deficit Based On Different Allocation Mechanisms

David L. Bijl[1] [ID], **Hester Biemans[2,3], Patrick W. Bogaart[1], Stefan C. Dekker[1,4], Jonathan C. Doelman[2], Elke Stehfest[2], and Detlef P. van Vuuren[1,2]**

[1]Copernicus Institute of Sustainable Development, Utrecht University, Utrecht, The Netherlands, [2]PBL Netherlands Environmental Assessment Agency, Den Haag, The Netherlands, [3]Water and Food Research Group, Wageningen University and Research, Wageningen, The Netherlands, [4]Faculty of Management, Science and Technology, Open University, Heerlen, The Netherlands

Abstract Freshwater scarcity is already an urgent problem in some areas but may increase significantly in the future. To assess future developments, we need to understand how future population growth, agricultural production patterns, energy use, economic development, and climate change may impact the global freshwater cycle. Integrated models provide opportunities for quantitative assessment. In this paper, we further integrate models of hydrology and economics, using the models IMAGE and LPJmL, with explicit accounting for (1) electricity, industry, and municipal and irrigation water use; (2) intersectoral water allocation rules at the 0.5° × 0.5°grid scale; and (3) withdrawal, consumption, and return flows. With the integration between hydrology and economy we are able to understand competition dynamics between the different freshwater users at the basin and grid scale. We run model projections for three Shared Socioeconomic Pathways (SSPs), more efficient water use, and no expansion of irrigated areas to understand the competition dynamics of these different allocation mechanisms. We conclude that (1) global water withdrawal is projected to increase by 12% in SSP-1, 26% in SSP-2, and 29% in SSP-3 during 2010–2050; (2) water deficits (demand minus allocated water) for nonagricultural uses are small in 2010 but become significant around 2050; (3) interannual variability of precipitation results in variability of water deficits; (4) water use efficiency improvements reduce water withdrawal but have little impact on water deficits; and (5) priority rules at the local level have a large effect on water deficits, whereas limiting the expansion of irrigation has virtually no effect.

1. Introduction

Freshwater scarcity is an urgent problem, among others, indicated by the alarming rates of groundwater depletion in different parts of the world (Dalin et al., 2017; Gleeson et al., 2012). For the future, several scenario studies project a further increase in water demand for irrigation, electricity generation, and industrial and municipal uses (Amarasinghe & Smakhtin, 2014; Bijl et al., 2016; Fujimori et al., 2016; Hejazi et al., 2014). These competing demands for freshwater are a key issue within the broader perspective of the food-water-energy nexus. Increasing water scarcity can also be caused by climate change (Gosling & Arnell, 2016; Schewe et al., 2014) and population growth in water-scarce areas (Arnell et al., 2011; Vorosmarty, 2000). While water scarcity occurs in different parts of the world, it is important to note that water scarcity is mostly a local phenomenon with important temporal characteristics (Hoekstra et al., 2012; Wada et al., 2011), although there are remote consequences as well, due to changes in food trade (Dermody et al., 2017). Given the interplay of these complex and uncertain factors, it is not immediately obvious where future water scarcity will arise.

In order to better assess the future development of freshwater scarcity, it is necessary to understand how future population growth, agricultural production patterns, energy use, economic development, and climate change may impact the global freshwater cycle. These complex interactions among water, food, energy, and climate call for integrative modeling tools. Most integrative approaches to date have focused on either (1) water demand and supply feedbacks at the aggregated region or basin level (Kim et al., 2016; Rosegrant et al., 2012; lacking some of the spatial hydrological detail within basins) or (2) analyses of the human impacts on the hydrological cycle (Alcamo et al., 2003; Wada et al., 2011; lacking some of the economic feedbacks such as trade and land use change). Hanasaki et al. (2013) developed a set of

integrative scenarios of water use for all sectors based on the Shared Socioeconomic Pathways (SSPs; O'Neill et al., 2014) and demonstrated that the socioeconomic scenarios and associated water use scenario dominate the impact of the water scarcity in the 21st century. Since then, different integrated model-based scenarios have been developed to understand the global water use and demand (Parkinson et al., 2016; Satoh et al., 2017; Wada et al., 2016), mostly using the SSP scenarios as their basis focusing on industrial use or, for instance, on coupled climate development impacts (Parkinson et al., 2016). These studies conclude that socioeconomic changes are the main drivers of water scarcity, for all SSP scenarios.

In this paper, we go one step further in integrating detailed hydrological and broader integrated assessment models (IAMs) by adding potential competition dynamics between the different freshwater users, at the basin and grid cell level. We use the IMAGE model (Stehfest et al., 2014) coupled to the crop growth and hydrological model LPJmL (Biemans et al., 2011; Bondeau et al., 2007; Gerten et al., 2011). This model setup includes full interactions among water availability, water demand, and other economic processes such as food demand, production, trade, and land use. We explicitly account for (1) water demand for the electricity, industry, and municipal sectors; (2) intersectoral water allocation rules at the 0.5° × 0.5° grid scale with a daily time step; and (3) including withdrawal (total water intake), consumption (e.g., evaporation), and return flows (withdrawal minus consumption). Besides simple priority rules to allocate water at the grid cell level (irrigation first versus other sectors first), we also investigate possible competition dynamics at the basin level (e.g., no irrigation expansion due to pressure from downstream nonagricultural water users). In our model we follow Hanasaki et al. (2008, 2013) and use water deficit as an impact metric defined as the difference between water demand and water allocated (see section 2.1.4). Thus, a water deficit means that not enough water is available to meet demand on a particular day for a 0.5° × 0.5° grid cell. In that case, water demand would remain unmet or could only be supplied by costlier and/or less sustainable means, which are not yet implemented in the model (e.g., nonrenewable groundwater; Döll et al., 2014; Wada et al., 2014b; desalination; or long-distance canals; Hanasaki et al., 2018, if possible at that location). We focus on water deficits for the nonagricultural sectors, since the value per m^3 of water is generally large compared to the value for irrigation use and because irrigation water shortages are dealt with internally in the model. We focus on "blue" water (fresh surface water or groundwater), not on "green" water (precipitation used by plants directly) or "gray" water (the volume of freshwater needed to sufficiently dilute polluted water).

The aim of this paper is (1) to understand how future water demand could develop, using consistent projections for different end-use sectors, (2) how supply-demand mismatches and nonagricultural water deficits could develop in the future, (3) the potential effects of strategies to reduce water deficits, and (4) how well IAMs can represent the complex dynamics between hydrological processes and competing water uses at a global scale. For this, we investigate how water supply and demand develop until 2050 using three very different socioeconomic scenarios, based on the SSPs (O'Neill et al., 2017; Riahi et al., 2017; Van Vuuren et al., 2017). These scenarios differ in terms of population growth, economic activity, lifestyle, and technological development. (The general scenarios do not include assumptions on specific technologies such as desalination and long-distance water transfer.) Strategies to reduce water deficits include efficiency improvements and water allocation rules. For the former, we compare the results of the "middle of the road" SSP-2 scenario with an SSP-2 variant (WaterEff) in which the water use efficiencies are improved. For the latter, we compare SSP-2 (in which the others sectors have priority) with an SSP-2 variant (IrrigFirst) prioritizing irrigation over other sectors, at grid cell level for daily time steps. Finally, we include another variant on SSP-2 (IrrigConst) without any irrigation expansion after 2005, to simulate the economic and/or political pressure that nonagricultural users may exert over water use in upstream areas. This gives some indication of how demand management at the watershed level may help safeguard an adequate water supply for downstream users.

In section 2, we first describe the water demand and supply model, followed by the scenario description. The resulting model projections in section 3 include future water demand and nonagricultural water deficits for the SSP scenarios, the effect of interannual variation in precipitation, the potential for additional water use efficiency improvements to alleviate water deficits, and the effects of different allocation mechanisms. In section 4, we put all the scenarios in perspective and discuss the current model and suggestions for further research. The main conclusions are presented in section 5.
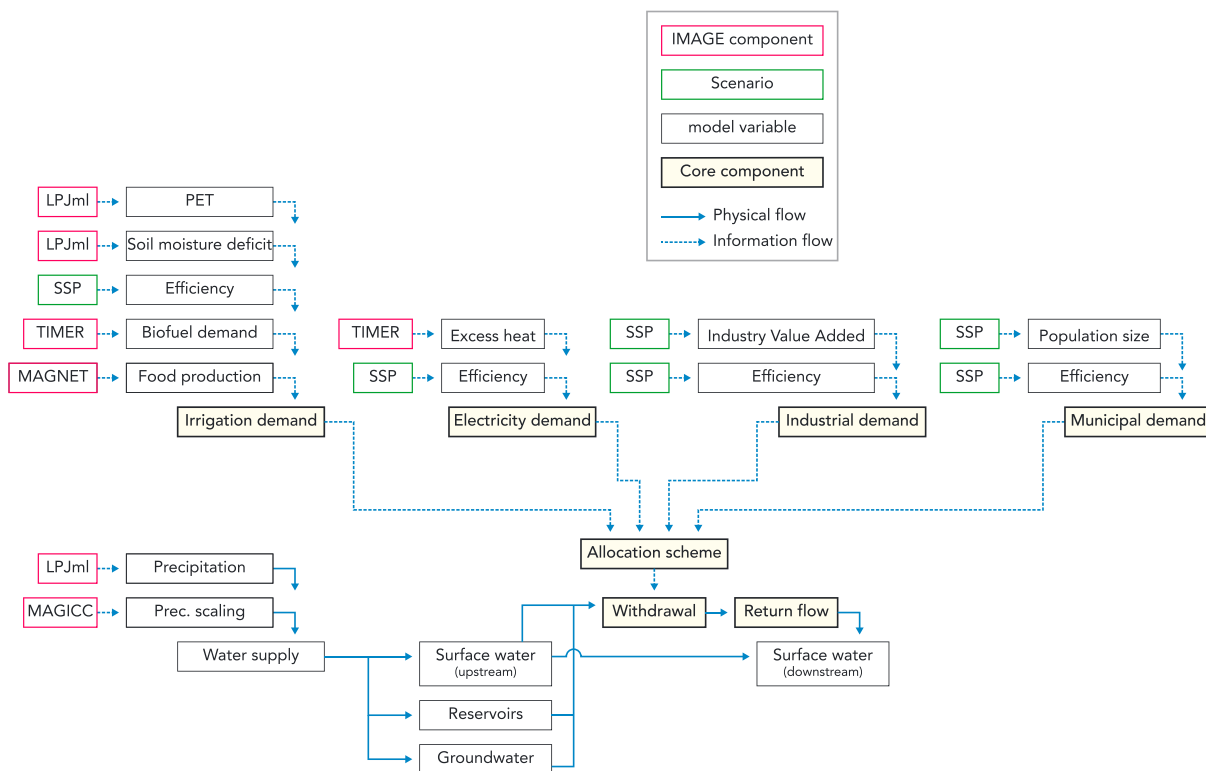
Figure 1. Water cycle flow chart indicating the various models and scenarios used in this study.

2. Methods

2.1. Model Setup

IMAGE is an IAM, describing key processes of global environmental change (Stehfest et al., 2014). The human system is represented in IMAGE with detailed models of energy demand and supply (TIMER), food demand (MAGNET), and agricultural production (TES). The Earth system includes, among others, the MAGICC climate model (Meinshausen et al., 2011) in combination with pattern scaling and the LPJmL global vegetation model (Bondeau et al., 2007). The LPJmL model includes the growth dynamics of natural vegetation and of food crops, as well as a process-based hydrological model. The major models are of the system dynamics type, in which the results for each time step influence the subsequent calculations. The time step is 1 year for IMAGE and its submodels and 1 day for LPJmL. The models are run for the period 1970–2100, but we focus on the changes between 2010 and 2050. Figure 1 shows the water cycle chart of all integrated models.

Given the spatial structure of the climate system and of human land use, there is large spatial variation in water supply and overall demand, as well as in the fraction of demand arising from the various water using sectors (irrigation, electricity, industry, and municipal). For this reason, water scarcity processes need to be studied with sufficient geographical detail. All water-related IMAGE-LPJmL processes are simulated at the $0.5° \times 0.5°$ grid scale at daily resolution. These include precipitation, land use, interception by vegetation, runoff, river routing, irrigation and nonagricultural demands, intersectoral allocation mechanisms, actual consumption/evapotranspiration, and return flows, as described below in more detail. For the 2010–2050 climate projections we used RCP 3.4 for SSP-1 and RCP 4.5 for SSP-2, SSP-3, and the other scenarios based on SSP-2. Larger-scale socioeconomic processes in IMAGE are modeled at the level of 26 regions, including population size, size and structure of the economy, energy demand, food demand, and technological development, using SSP-1, SSP-2, and SSP-3.

The 26 regions include several large countries and the following aggregate regions:

- Rest of Central America: everything except Mexico.

- Rest of South America: everything except Brazil.
- Western Europe: Scandinavia, Austria, and everything to its west, plus Greece.
- Central Europe: the Baltic states, Poland, Czech Republic, Slovakia, Hungary, Romania, Bulgaria, and the smaller Balkan states.
- Ukraine region: Ukraine, Belarus, and Moldova.
- Northern Africa: Western Sahara, Morocco, Algeria, Tunisia, Libya, and Egypt.
- Western Africa: Chad, Central African Republic, the Democratic Republic of the Congo, and everything to their west.
- Eastern Africa: Sudan, South Sudan, Uganda, and everything to their west, plus Rwanda, Burundi, and Madagascar.
- Rest of Southern Africa: Angola, Zambia, Tanzania, and everything to their south, except for the country South Africa.
- Middle East: Syria, Iran, Yemen, and everything in between.
- Russia: includes Georgia, Armenia, and Azerbaijan.
- Kazakhstan region: includes Uzbekistan, Turkmenistan, Kyrgyzstan, and Tajikistan.
- China: includes Mongolia and Taiwan.
- Rest of Southern Asia: Afghanistan, Pakistan, Nepal, Bhutan, Bangladesh, Sri Lanka, and the Maldives.
- South East Asia: everything from Myanmar to the Philippines.
- Indonesia: includes Papua New Guinea.
- Oceania: Australia, New Zealand, and all the small islands to their northeast.

2.1.1. Water Demand

The key water demand sectors are irrigation, electricity, industry, and municipal use, which are all covered in the projections presented here. Water demand for livestock is not included because it is comparatively small. Water use for energy extraction/refining is also comparatively small and is included in the industry sector. Evaporation from hydropower reservoirs is included for the dams in the GRanD database (Lehner et al., 2011), but dams to be built in the future are not included in the model.

In IMAGE, the irrigation water demand ultimately depends on demand for food (crops and animals). Food demand is based on historical data from FAO (FAOSTAT, 2016) and future changes using price and income elasticities from the computable general equilibrium model MAGNET (Woltjer et al., 2014). Food production also includes animal feed, and the feed mix and feed efficiency are scenario dependent. Demand for biofuel crops is calculated in TIMER, the energy model within IMAGE. The seven food crop groups in IMAGE can be produced by both irrigated and rainfed agriculture, whereas grassland and the four bioenergy crops are assumed to be only grown under rain-fed conditions. The locations of cropland expansion and crop distribution are determined by an algorithm, which takes into account the potential yields per crop, distance to major cities, population density, and topography. The resulting yields depend on climate and soil characteristics (at grid cell level) and technology/management factors. The change in total area of land per region equipped for irrigation differs per SSP scenario. Within the regions, locations of irrigated agriculture are based on proximity to existing irrigation, potential production increase, and water availability. The cropwater demand for irrigation depends on the soil moisture deficit and atmospheric evaporative demand and is estimated daily in LPJmL (Bondeau et al., 2007). The irrigation scheme is described in detail by Rost et al. (2008) and includes the option to take water from nearby reservoirs (Biemans et al., 2011). To calculate the total water withdrawal demand for irrigation, the crop demands are divided by country specific irrigation efficiencies. Those irrigation efficiencies (ratio between water needed by the crops and actual withdrawal) improve gradually over time, depending on the region and SSP scenario.

Nonagricultural water demand is modeled separately for the electricity, industry, and municipal sectors, in terms of both withdrawal and consumption (Bijl et al., 2016). The drivers for demand in the respective sectors are excess heat from thermo-electric power plants, industry value added in dollar terms, and population size, with technological innovation for potential efficiency improvements in each sector. Nonagricultural demand is computed for the 26 IMAGE regions and is downscaled to a 0.5° × 0.5° resolution grid, weighted by the percentage of the region's population in each cell (Klein Goldewijk et al., 2010), using the SSP population development (KC & Lutz, 2017). The nonagricultural demand is kept constant throughout the year in the current implementation.

2.1.2. Water Availability

Water availability and use at the grid cell level and daily time step are computed in LPJmL. Both temperature and precipitation in the model vary by year, season, and geographic location. This is done by calculating global mean temperature on the basis of the emission trajectory using the simple climate model MAGICC. The daily and geographically explicit precipitation and temperature patterns are subsequently derived using pattern scaling with the HadCM3 climate pattern (IPCC-DDC, 2007). The interannual variation of precipitation is modeled by calculating the historical variation from the mean for 1970–2000 (Climatic Research Unit, 2017) and adding this pattern to the projected value. Climate change influences the growth of both natural vegetation and crops via temperature and precipitation, but not via CO_2 fertilization. In turn, both natural vegetation and crops influence interception, infiltration, evapotranspiration, and runoff, which contributes to surface water availability. Thus, irrigation water use and the surface water availability vary day to day, whereas nonagricultural water demand does not.

Irrigation water demand within a specific grid cell can be supplied from surface water (streams and lakes) in the same cell, the directly neighboring cell with the highest discharge, or nearby artificial reservoirs (at a higher altitude and upstream on the same river or a river within five-cell distance). The reservoir operating scheme combines features from Hanasaki et al. (2006) and Haddeland et al. (2006), with the important modification that the minimum release is set at 10% of mean monthly inflow, so that more water is stored for irrigation in dry seasons (Biemans et al., 2011). Although groundwater is used for nonagricultural purposes in many locations, the current model allows nonagricultural sectors to only use local surface water in streams and lakes to fulfill their demand. However, unmet demand for the nonagricultural sectors may still be fulfilled if sufficient water becomes available within 30 days. This mechanism simulates short-term local water storage (e.g., small underground reservoirs, rooftop tanks, the municipal water system, water treatment facilities, or artificial lakes) and was included so that short-term supply variability does not immediately cause a water deficit (Rost et al., 2008). However, its effects are also visible right after the end of a prolonged period of water shortage and in that case can be interpreted as fulfillment of postponed demands and/or a replenishing of depleted short-term storage facilities.

Available water from the various sources is allocated to the various sectors' demands by the allocation scheme (described below). The allocation scheme operates on withdrawal demand: if nonagricultural withdrawal demand cannot be met, their consumption is reduced proportionally. For irrigation, consumption (evapotranspiration) is calculated dynamically. Return flows (withdrawal minus consumption) from irrigation and other sectors are added back into surface water and routed to downstream cells. Note that environmental flow requirements are presently not included in the LPJmL model as a strict limit, nor are they always firmly protected in practice. The reservoirs in LPJmL do release at minimum 10% of their mean monthly inflow, but this water is not protected from consumption by other users downstream.

2.1.3. Water Allocation Mechanisms

If water supply is scarce compared to demand, the question how water is allocated becomes important. A wide variety of allocation mechanisms is used in practice. Nonprice mechanisms include rights to fixed volume quotas and rights to percentage shares of available water, often arising from traditional agricultural arrangements (Johansson et al., 2002; Molle & Berkoff, 2009). Prices do play a role in some areas, but their effects are generally limited to behavior within a sector. Intersectoral allocation can theoretically be affected via price-induced efficiency, but this is rare because water prices are generally low compared to other inputs (Bos & Wolters, 1990). Irrigation water is generally 100 times cheaper than water used in other sectors (Kim et al., 2016), but such average water prices convey little information anyway (Molle & Berkoff, 2009). Thus, intersectoral water allocation is governed mostly by priority rules and not as much by prices.

Other IAMs and large-scale hydrological models have implemented water allocation among economic sectors in different ways. For instance, the IMPACT model gives priority to domestic, industry (including electricity), and livestock water uses before irrigation, at the scale of 281 intersections of country borders with river basins (Rosegrant et al., 2012). GCAM model reconciles agricultural, energy, and industrial and municipal sector water demand with water availability in 235 river basins at an annual time step, based on relative prices and price-induced demand reduction (i.e., price elasticities; Kim et al., 2016).

Here available water is allocated to the sectoral demands at the local scale (grid cells) and daily time step. We use existing priority-based allocation mechanisms in LPJmL; that is, one sector can have all its demand met

before the next sector gets its chance, until all available water is allocated or all demands are fulfilled. Although nonagricultural water demand consists of three sectors (electricity, industry, and municipal), the main issue explored in this paper is water allocation between irrigation and nonagricultural uses. The default allocation mechanism is "OtherFirst," in which nonagricultural demands are fulfilled before irrigation. This is in line with the existing situation in many places. In "IrrigFirst," irrigation is prioritized, to explore what happens if an alternative allocation rule is used. Although we have no specific examples of irrigation receiving priority access above other users in the same location, this situation could occur if farmers have strong irrigation rights or if the location of canals gives them de facto priority access. Note that all upstream users (both agricultural and others) are automatically favored over all downstream users, since the prioritization happens within cells only.

An important innovation in this research is that we allocate water withdrawal between sectors. Often, consumption is used for determining the total extraction of water from a river, since this is the part of withdrawal that is not returned in the river. However, that simplification only works if the available volume of water is larger than the total withdrawal demand, which is not always the case. In this paper, we assume that if the withdrawal volume allocated to the nonagricultural sectors is smaller than their demand, part of this withdrawal demand is unmet and therefore actual consumption is decreased proportionally. In LPJmL, the return flow from irrigation goes back into the river routing scheme and is no longer available in the same grid cell and time step. Now nonagricultural withdrawal and return flow have been added. The main benefit of this approach of allocating withdrawal rather than consumption is that it more accurately reflects the limiting effects of water scarcity, especially regarding electricity generation using once-through cooling (with high withdrawal and low consumption rates). Many industrial processes also withdraw large quantities of water and consume (evaporate) a more or less fixed fraction of that.

2.1.4. Water Scarcity, Water Deficit, and Feedback Effects

In this paper we measure water deficit instead of water scarcity. Water scarcity (water demand divided by availability) can be a useful metric at the aggregate level (basin or region per month or year). However, actual water use and availability happen within grid cells and vary widely between grid cells and between days. Although water scarcity can easily be calculated for a single grid cell, the metric goes to infinity when water availability at any day approaches zero (which would rarely happen at the aggregate level). This problem can be dealt with by capping the water scarcity metric at some level (e.g., 1.0 means demand equals availability) and labeling anything above it as "extremely scarce." However, the metric would then be most inaccurate at precisely the most interesting points, that is, when availability is small relative to demand. Therefore, water deficit is a more suitable metric to calculate.

The amount of water allocated to irrigation affects the local production in the grid cell, calculated by the crop growth model. The actual water consumption for irrigation is calculated on a grid cell basis and depends on water availability. This means that water scarcity for irrigation in the IMAGE calculation is not expressed as a water deficit but as a reduction of crop production. The yields per grid cell also influence the extent and location of crops planted in the next year according to the land use allocation algorithm. The expansion of irrigated areas (prescribed per scenario and region) is allocated to specific grid cells based on water availability and the added value that irrigation would have.

For the nonagricultural sectors, we represent impacts in terms of water deficit (m^3), recorded for each day and grid cell as the difference between the water withdrawal demand and the actual (allocated) water withdrawal:

$$d_i(t) = D_i(t) - S_i(t) \tag{1}$$

where d denotes water withdrawal deficit (m^3) in cell i on day t, D is demand for water withdrawal (m^3), and S is water availability (m^3).

Relative water deficit is the deficit as percentage of demand:

$$d_i^{rel}(t) = \frac{d_i(t)}{D_i(t)} \times 100\% \tag{2}$$

Where d^{rel} indicates relative water deficit (%) in cell i on day t, d is the absolute water withdrawal deficit (m^3),

and D is demand for water withdrawal (m³). Since nonagricultural water consumption is decreased by the same proportion as withdrawal, the relative water deficit is the same for withdrawal and consumption.

Both indicators relate to economic impacts such as lost power generation capacity or lost industrial output. However, we have not yet implemented a feedback mechanism by which the electricity, industry, and municipal sectors in each grid cell reduce their future water demand after experiencing water deficits (either by locally reducing the associated economic activity or by using more water-efficient technology/management). Also note that in LPJmL, nonagricultural users can only take surface water from their own grid cell and their neighbor. Thus, deficits could also be interpreted as a need to increase the water supply from groundwater, desalination, or long-distance canals connected to other grid cells or upstream reservoirs. Such measures can be costly and/or less sustainable, and their feasibility depends on the local situation.

2.2. Scenario Specification

The SSPs are a recently developed scenario framework to study potential future economic, demographic, and technological developments (Riahi et al., 2017). The storylines are described in O'Neill et al. (2017) and quantified for population (KC & Lutz, 2017) and income (Dellink et al., 2017). We focus here on the SSP-1, SSP-2, and SSP-3 as implemented in the IMAGE model (Van Vuuren et al., 2017). Assumptions regarding technological and lifestyle factors were made in line with the SSP story lines (see Table 1).

In addition to three different socioeconomic pathways, we explore scenarios in which we vary the allocation rules and water use efficiency while keeping socioeconomic drivers as in SSP-2 (Table 2).

To investigate the potential impact of different allocation mechanisms, we run the middle of the road SSP-2 scenario for two additional scenarios. The default priority rule gives priority to nonagricultural uses (OtherFirst), and the alternative priority rule favors irrigation (IrrigFirst). These priority rules take effect at the grid cell level and daily time step but may have indirect effects downstream as well (since the return flows differ per sector). A second scenario (IrrigConst) is added to investigate whether nonagricultural sectors can reduce their water deficits compared to SSP-2, by using economic and/or political pressure to limit irrigation water use upstream. In this scenario, we explore a rather stringent case by keeping the irrigated land area constant at 2005 levels and locations, while the nonagricultural sectors also have priority access at the local level.

To estimate the potential effects of increased water efficiency (WaterEff), we run SSP-2 with the default allocation rule OtherFirst but follow SSP-1 regarding faster irrigation and nonagricultural efficiency improvements and more water-efficient power plant cooling systems.

3. Results

3.1. Spatial and Temporal Detail

To correctly interpret the aggregated results presented in the subsequent sections, it is necessary to first understand the model calculations on a more detailed level. We illustrate this in Figure 2, using the Jordan river as an example.

Figure 2 shows how the model results were calculated (for 2010, in SSP-2, with the OtherFirst allocation mechanism). The map (top panel) shows the 0.5° × 0.5° grid cells. The color indicates whether irrigation (green) or nonagricultural demand (red) is dominant. Cells with low total withdrawal (irrigation + nonagriculture) are more transparent. Demand for the nonagricultural sectors is indicated by the size of the circles in each cell. The water drainage direction is indicated by the arrows, with dark blue arrows representing relatively high discharge flowing out of the cell (hm³/day, annual average). Note that each cell can receive water from multiple cells but can only drain into one other cell. The view is centered on the Jordan river and its tributaries. The cells numbered 1–4 correspond to the four lower panels, which show the monthly pattern (in 2010) of demand, allocation, return flow, and discharge in each cell. Note that the model computes these values for each day but only stores the monthly aggregates to keep file sizes manageable.

Irrigation and discharge are highest in cell 1 (as can also be seen from the map) and are much larger than nonagricultural water demand for the period February–August. In September and October, the water flows are suddenly reduced and result in deficits. From the map, we can see that there are no cells draining into

Table 1
Overview of SSP Scenarios (Based On Previous Work)

	SSP-1	SSP-2	SSP-3
Description	A world oriented at sustainable development, global cooperation, less inequality, rapid development of environmentally friendly technologies, low population growth, and high GDP per capita	A middle of the road scenario in between SSP-1 and SSP-3 on most dimensions	A "fragmentation" scenario with rapid population growth, reduced trade and cooperation, slower technological development, and related much lower GDP per capita and larger differences between regions
Population growth	Peak around 8.5 billion in 2050	Peak around 9.5 billion in 2070	Around 13 billion in 2100 and increasing
Average income	Increases to 85,000 in 2100	Increases to 60,000 in 2100	Increases to 25,000 in 2100, with larger regional differences
Industry value added	Increases to 92×10^{12} IVA\$ in 2100	Increases to 119×10^{12} IVA\$ in 2100	Increases to 51×10^{12} IVA\$ in 2100
Electricity production	Peak around 280 EJ/year in 2090	Around 380 EJ/year in 2100 and still increasing	Around 290 EJ/year in 2100 and still increasing
Electricity technologies	More natural gas and wind power (offshore and onshore)	Mostly coal (transitioning to combined cycle), some natural gas, wind, hydropower, and nuclear	More conventional coal, less wind power
Mix of cooling systems	Full adaptation: shift from once-through to seawater, wet tower, or dry tower cooling[a]	50% of feasible adaptation is realized.	No adaptation, cooling systems remain unchanged
Wet tower water efficiency	Toward 55.9% (withdrawal) and 50.4% (consumption) less water use in 2040	Half the water savings of SSP-1	No water savings
Industrial water efficiency	Save 1.05–3.33%[b] per year (withdrawal) and 1% (consumption)[c]	Save 0.55–2.84%[b] per year (withdrawal) and 0.5% (consumption)	Save 0.05–2.35%[b] per year (withdrawal) and 0% (consumption)
Municipal water efficiency	Save 0.73% per year (withdrawal) and 0.85% (consumption)[c]	Save 0.48% per year (withdrawal) and 0.49% (consumption)	Save 0.28% per year (withdrawal) and 0.22% (consumption)
Irrigated area	Irrigated area growth rate is 50% lower than in SSP-2	Irrigated harvested area increases follow FAO agricultural outlook	Irrigated area growth rate is 50% higher than in SSP-2
Irrigation efficiency	After 2006, each year 0.1% of the remaining irrigation efficiency gap is closed in all regions. This "gap" is the difference between the current efficiency factor (e.g., 0.7) and 100% efficiency (i.e., 1.0)	Efficiency for newly irrigated areas improves 0.2%/yr (resulting in an average gap closure rate of 0.04% per year)	Irrigation efficiency remains at current levels
Priority rule	OtherFirst	OtherFirst	OtherFirst
Climate projection	RCP 3.4	RCP 4.5	RCP 4.5

Note. Source: Bijl et al. (2016), Doelman et al. (2018), and Van Vuuren et al. (2017).
[a]Adaptation to the extent deemed feasible in light of regional climate, coastline access, and power generation technologies (Bijl et al., 2016). [b]We assume that regions with a low consumption-withdrawal ratio have more room for improving withdrawal efficiency by recycling water on premises (which would subsequently increase the consumption-withdrawal ratio since additional water is consumed in every cycle). [c]Industrial efficiency improvements are based on the current consumption-withdrawal ratio, an assumed maximum ratio of 75% in 2100, and, for consumption efficiency, the assumed industrial energy efficiency improvements in TIMER. Municipal efficiency improvements are based on the most water-efficient appliances currently available, market penetration rates in 2100 of 75–100% for SSP-1, 50–80% for SSP-2, and 25–60% for SSP-3, and the current share of specific uses in households (Mayer et al., 1999), then converting the difference between 2011 and 2100 to an average annual improvement percentage. See sections 2.5.2 and 2.5.3 in Bijl et al., 2016).

Table 2
Additional Scenarios Deviating From SSP-2

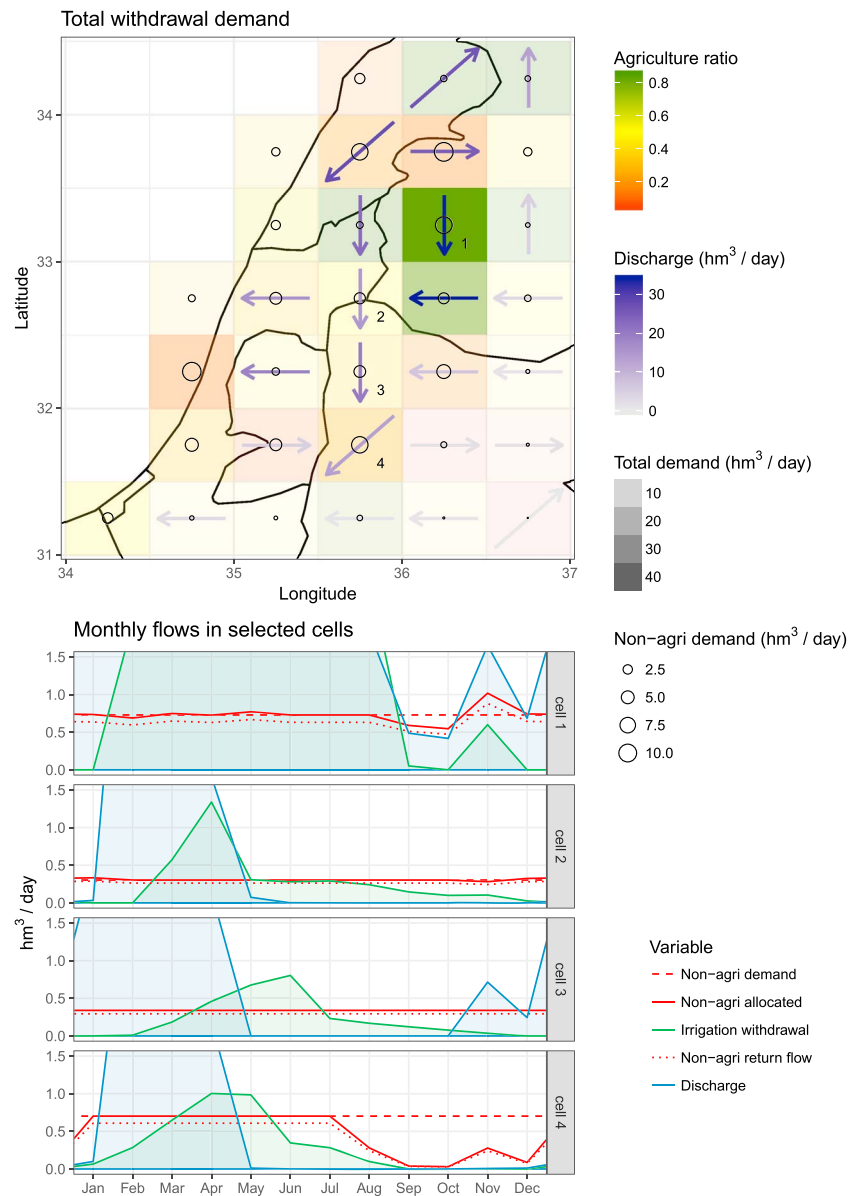|	IrrigFirst	IrrigConst	WaterEff
Description	Irrigation gets priority before other sectors.	No expansion of irrigated areas after 2005	Higher water use efficiencies in all sectors
Socioeconomic scenario	SSP-2	SSP-2	SSP-2
Climate projection	RCP 4.5	RCP 4.5	RCP 4.5
Priority rule	IrrigFirst	OtherFirst	OtherFirst
Other assumptions		Irrigated areas remain fixed after 2005. Irrigation water use slowly declines due to SSP-2 irrigation efficiency improvements.	Faster efficiency improvement in irrigation and nonagricultural water uses, as in SSP-1 (see Table 1). However, power generation technologies remain the same as in SSP-2.

Figure 2. Spatial and temporal detail in model calculations (for explanation see the text).

cell 1, which is therefore solely dependent on precipitation. The bottom panel for cell 1 shows how the deficit and other variables are calculated. In September and October, apparently, there is not enough water to satisfy the nonagricultural demand (water availability before allocation is not shown, but water allocated to nonagricultural sectors is lower than their demand). Since the allocation rule is OtherFirst, there is no water left for irrigation. Return flows from the nonagricultural sectors are almost as high as the water allocated to them, which means that the withdrawn water flows through the industrial, municipal, and power plant cooling systems but only a small fraction of that water is consumed (evaporated). Since the discharge shown in the panel is as large as the nonagricultural return flows, the discharge out of the cell consists entirely of return flows from the nonagricultural sectors during these two months. In November, the volume allocated to the nonagricultural sectors is higher than their demand. This "negative deficit" simulates the fulfillment of postponed demands and/or replenishment of local short-term water storage facilities (see section 2.1.3).

The discharge from cell 1 flows to cell 2 and then cell 3, but the patterns do not match exactly since other cells also drain into cell 2 and cell 3 (as shown in the map). From May onward, there is only

barely enough water in cells 2 and 3 to satisfy nonagricultural demands, with very little left for irrigation. Cell 4 receives water mainly from cell 3, besides local precipitation and very small flows from the cell to the west. This results in severe water deficits during August–December. In November–December, the pattern of discharge from cell 3 is clearly reflected in the pattern of water allocated to the nonagricultural sectors in cell 4. Note that the volumes do not match exactly, because every cell can also source water from its direct neighbors. For instance, in November and December, not all the discharge from cell 3 (blue line) is allocated to end users in cell 4 (red line; although they could clearly use more water) but is partly distributed to neighboring cells. The reverse can be seen in June and July, when nonagricultural demands are still satisfied in cell 4 (red line) although there is no discharge from cell 3 (blue line): the additional water is supplied by neighboring cells. Although the sharing of water between neighboring cells (in times of shortage) has a spatially smoothing effect, the effect of upstream cells on those downstream is clearly visible.

3.2. Water Demand and Deficit Under the SSP Scenarios

The scenarios are calculated for each year, and the results in 1 year influence the calculations for subsequent years. Here we focus on the resulting differences between 2010 and 2050, in terms of water withdrawal for SSP-1, SSP-2, and SSP-3 (Figure 3). At the global level, water withdrawal increases significantly for all SSPs: 12% in SSP-1, 26% in SSP-2, and 29% in SSP-3. All scenarios show increasing water withdrawal in the municipal sector: 311–366 additional km^3/yr. Water withdrawal for electricity generation increases in SSP-2 (+221 km^3/yr) and SSP-3 (+303 km^3/yr). Irrigation water withdrawal increases mainly in SSP-3 (+270 km^3/yr including conveyance losses).

The regions with largest water withdrawal are China and India. In both regions, and especially in India, water withdrawal is projected to increase even further. The projections for India show little difference across the SSPs (46–56% increase), partly because the effects of population growth and income work in opposite directions: SSP-1 has higher income growth (and thus more resource use per capita), but lower population growth. By contrast, SSP-3 is characterized by lower income growth (thus lower resource use per capita), but higher population growth. Disregarding efficiency gains, this mechanism is at work in all regions but is most clearly visible for India and the four African regions because here both income and population are projected to grow significantly. In China, growing withdrawal demand is mostly due to electricity generation (22% increase in SSP-1, 83% in SSP-2, and 97% in SSP-3). This is also the reason that SSP-1 shows much lower withdrawal in 2050 compared to SSP-2 and SSP-3 in China: a combination of higher-energy efficiency and a larger share of electricity from solar and wind.

The USA is the third largest region regarding water withdrawal in 2010, but here withdrawal is projected to drop due to decreasing water use in industry and electricity generation, especially in SSP-1.Very similar water use patterns are projected for Western Europe (5th in magnitude) and Russia (8th).

Many developing regions show increasing water withdrawal in all scenarios, with the least increase for SSP-1 and the highest increase for SSP-3 (Rest Southern Asia, Rest Southern America, Kazakhstan region, Mexico, Northern Africa, and Southeast Asia). In these cases, the main differentiating factors are the efficiency improvements in the irrigation and electricity sectors, which are high in SSP-1 and low in SSP-3. For other developing regions, rapid increases in water withdrawal are projected for all SSPs, both in absolute terms and relative to 2010 (Indonesia, Eastern Africa, Western Africa, and rest of Southern Africa). In these cases, the main increase comes from municipal water demand, which is high in SSP-3 due to population growth and high in SSP-1 due to increasing income.

At the annual level, the relative water deficit is the ratio of the nonagricultural deficit divided by the nonagricultural demand (in Figure 3, the red bar divided by the sum of the pink, gray, and orange bars). Annual water deficits in 2050 occur mostly in India (7–8% of nonagricultural demand), rest of Southern Asia (6–7%), Mexico (9–11%), Northern Africa (12–13%), and the Middle East (20–22%). These deficits are a clear indicators of water scarcity, although the remaining demand might still be met from groundwater, long-distance canals, or desalination (since nonagricultural sectors cannot use these water sources in the current model implementation). These annual numbers are the sum of daily deficits. Looking at the monthly level, it becomes clear that water deficits are highly seasonal in nature and can be problematic even when they are small at the annual level (Figure 4).
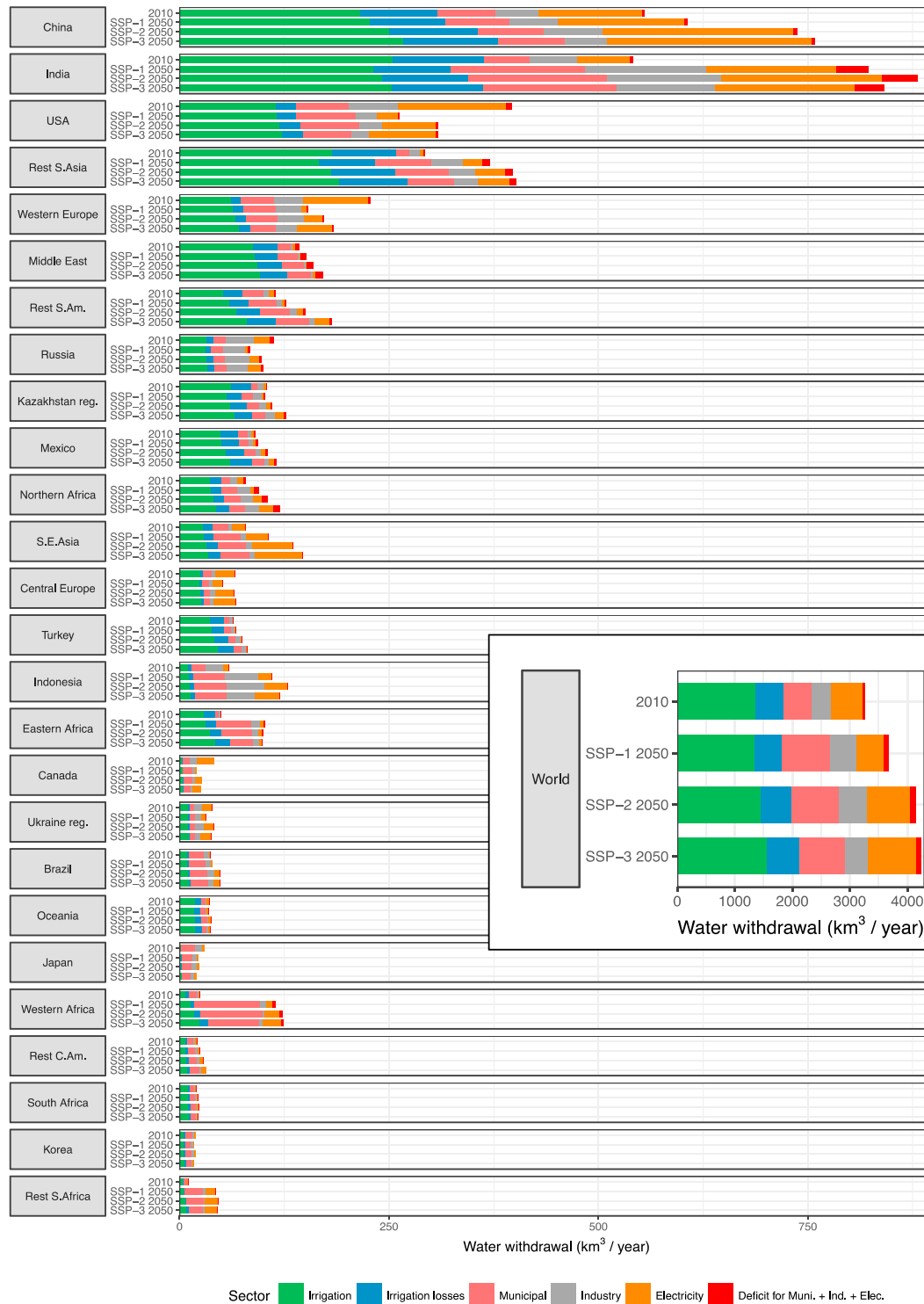
Figure 3. Historical (2010) and future projections for three SSP scenarios (2050) of water withdrawal (km^3/yr) per region and economic sector. To reduce the effect of interannual variation, the 2010 and 2050 values are 5-year averages. Regions are sorted from high to low total water withdrawal in 2010, and the global aggregate is shown in a separate frame. The values shown are the allocated water withdrawal, and the deficit (in red) is the difference between the withdrawal demand and allocated withdrawal volume for the nonagricultural sectors (municipal, industry, and electricity combined), under the default allocation mechanism OtherFirst.
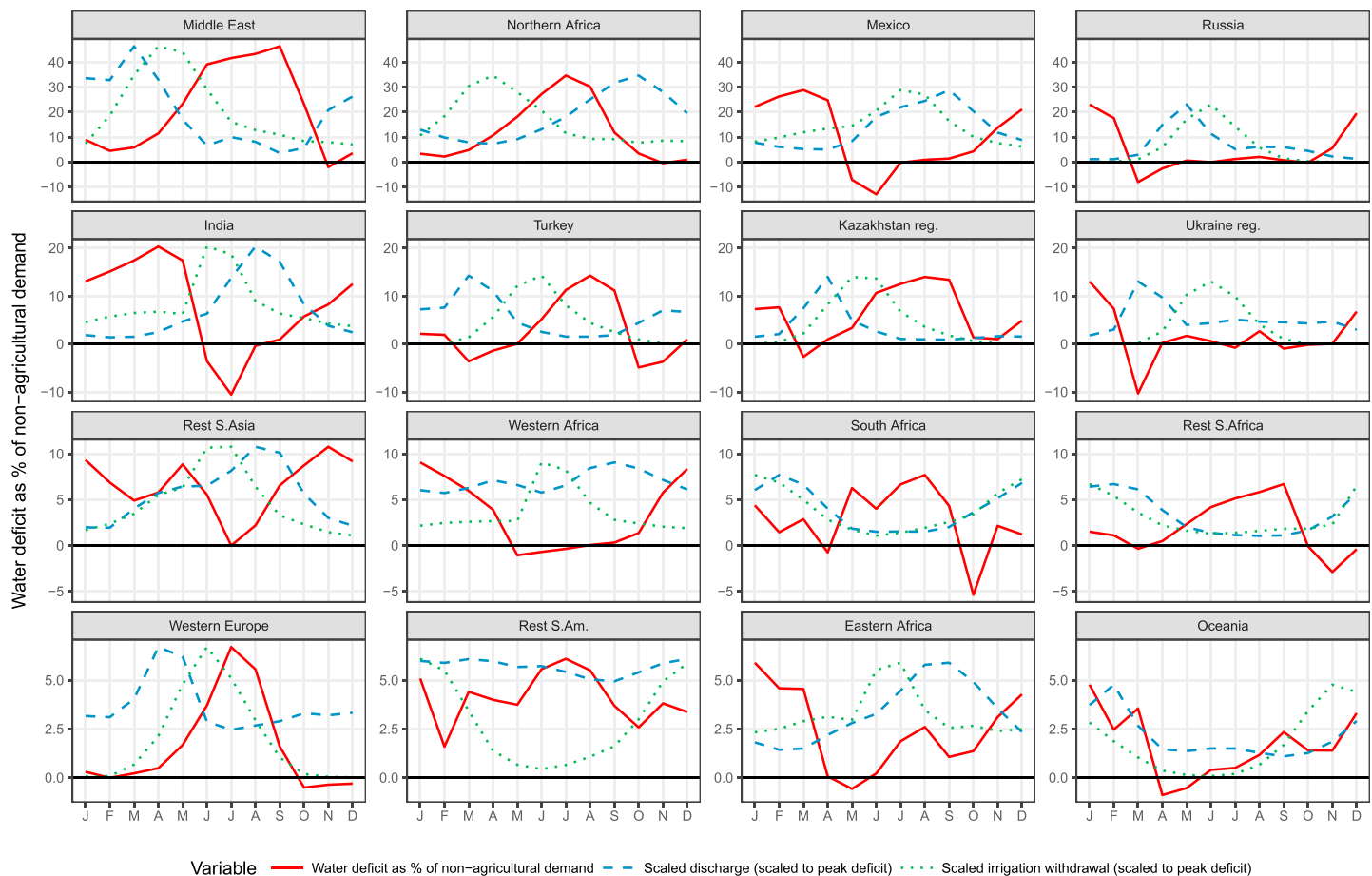
Figure 4. Nonagricultural water deficit as % of demand (red line) per month under SSP-2 (average 2045–2055). Discharge (blue dashes) and withdrawal allocated to irrigation (green dots) are only provided for context and are scaled so that their peak matches the peak of relative deficit in each region. The regions are sorted from high to low peak monthly deficit (showing only 16 of the 26 regions). These relative deficits apply to both withdrawal and consumption (see section 2.1.4). A negative deficit (higher allocation than demand) signifies replenishing of short-term water storage facilities. The y axis is different for each row of panels but the same for the regions within a row.

At the monthly level, very high relative water deficits are projected for 2045–2055 in two regions: the Middle East and Northern Africa. Here peak monthly water deficit surpasses 40% and 30% of demand, respectively. The water deficits last for many consecutive months, and the water supply in the most water-abundant months is not enough to replenish short-term water storage and compensate for some of the deficits.

Water deficits are also high, but temporary, in December in Russia (23%) and the Ukraine region (13%; including Belarus and Moldova). These deficits are caused by low runoff due to freezing in winter and are partly compensated by the spring melt in March.

The influence of the monsoon can be seen in India and to some extent in the rest of Southern Asia: water deficits increase in the autumn and winter up to 20% (India) and 10% (rest of Southern Asia), until the monsoon rains suddenly bring plenty of water in May, June, and July. Note that there is a lag between major precipitation events and the peak discharge shown in Figure 4. Since the region "rest of Southern Asia" is geographically diverse and includes dry Afghanistan and Pakistan, wet Bangladesh, and mountainous Nepal, the pattern is less clear. The monsoon is strongest in the east, and Nepal has runoff from the snowmelt in spring. Mexico also shows a pattern very similar to India, with deficits of 20–30% during January–April and partial compensation in May and June.

Projected deficits for nonagricultural sectors seem to be related to irrigation for Western Europe, Turkey, and the Kazakhstan region (which includes Kyrgyzstan, Tajikistan, Turkmenistan, and Uzbekistan). Between March and September, irrigation increases while overall streamflow decreases, causing water deficits for densely
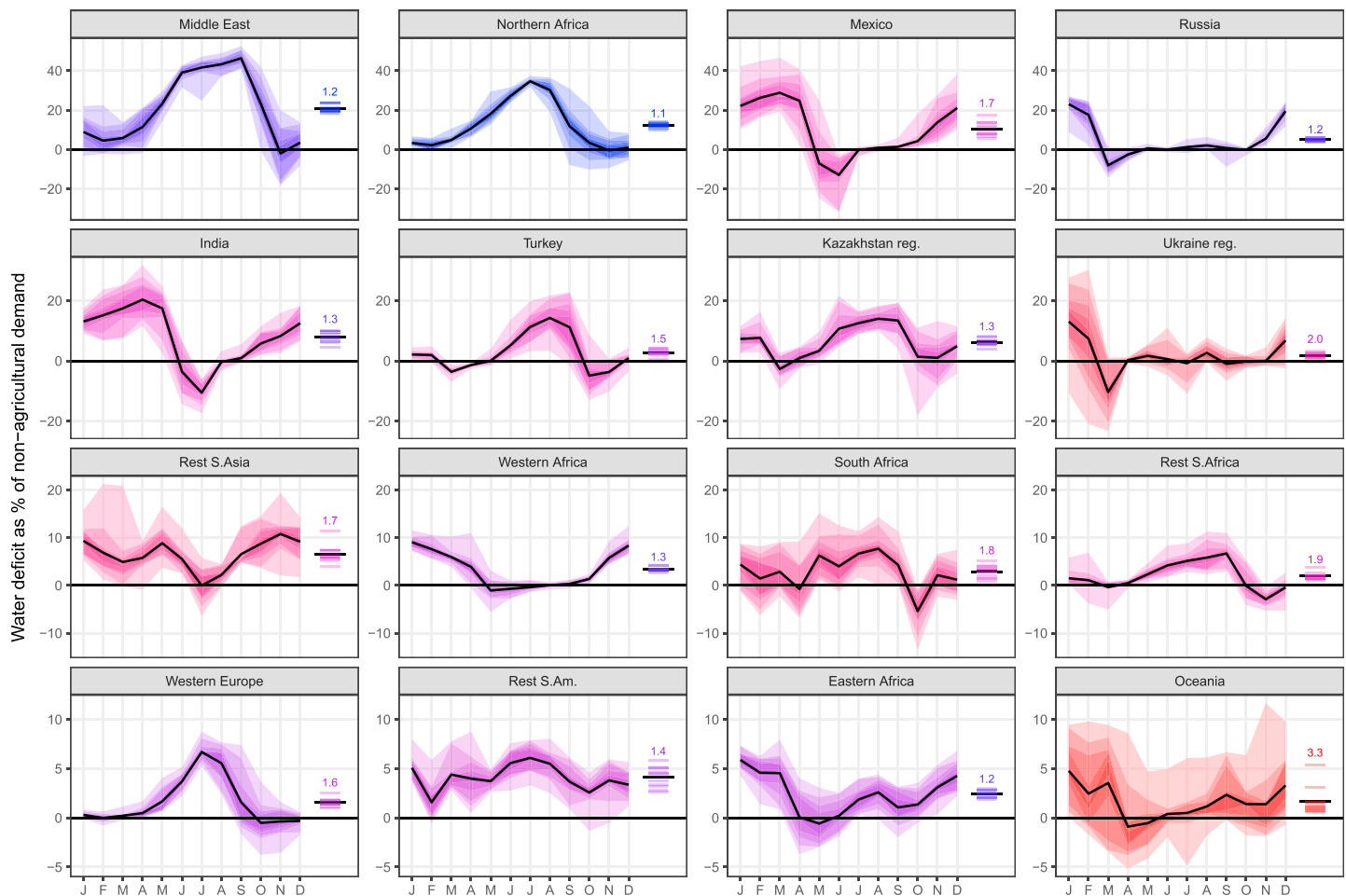
Figure 5. Interannual variation of nonagricultural water deficit as % of demand for 2045–2055, per region and per month under SSP-2. When the line is below 0, there is a "negative deficit" or surplus of water, which can be interpreted as either fulfillment of postponed demand or replenishment of temporary local water storage (section 2.1.3). The black line is the average of the 11 years, calculated separately for each month. The shaded areas indicate the bandwith of the data for each separate month (thus the data within the more narrow bandwiths do not necessarily belong to the same year). The regions are the same as in Figure 4. The net annual deficit (sum of monthly deficits and compensating surpluses) for each year is shown by the colored lines on the right; the black line is again the average of these, and the number on the right is the ratio of the highest occurring net annual deficit to the average. The color blue indicates that all years are close to the average, whereas red indicates that the water deficit in a specific year can be much higher than the average over the years.

populated areas downstream from May onward. As soon as the crops are harvested and the autumn rains come, the deficit is quickly reduced and partly compensated in October and November (via the mechanism for postponed demand fulfillment or short-term storage replenishment). Management at the watershed level could probably prevent water deficits for nonagricultural users, but these results are still indicative of water competition and scarcity issues.

3.3. Interannual Variation of Water Deficits

Precipitation may vary substantially from year to year and therefore may have a large impact on water deficits. Therefore, we investigate the variation of water deficits over the years 2045–2055, in terms of both seasonal patterns and net annual deficits (Figure 5).

Figure 5 shows that the regions with the highest peak monthly deficit, the Middle East and Northern Africa, are projected to experience these peak deficits fairly consistently from year to year. For Mexico, however, peak deficits can reach 41–47% in January–April in some years, whereas the average is 22–29%. Whereas Russia and the Ukraine region have very similar seasonal deficit patterns, the potential for negative surprises is much larger in Ukraine region: the highest peak monthly deficit in 11 years there is 30% compared to an
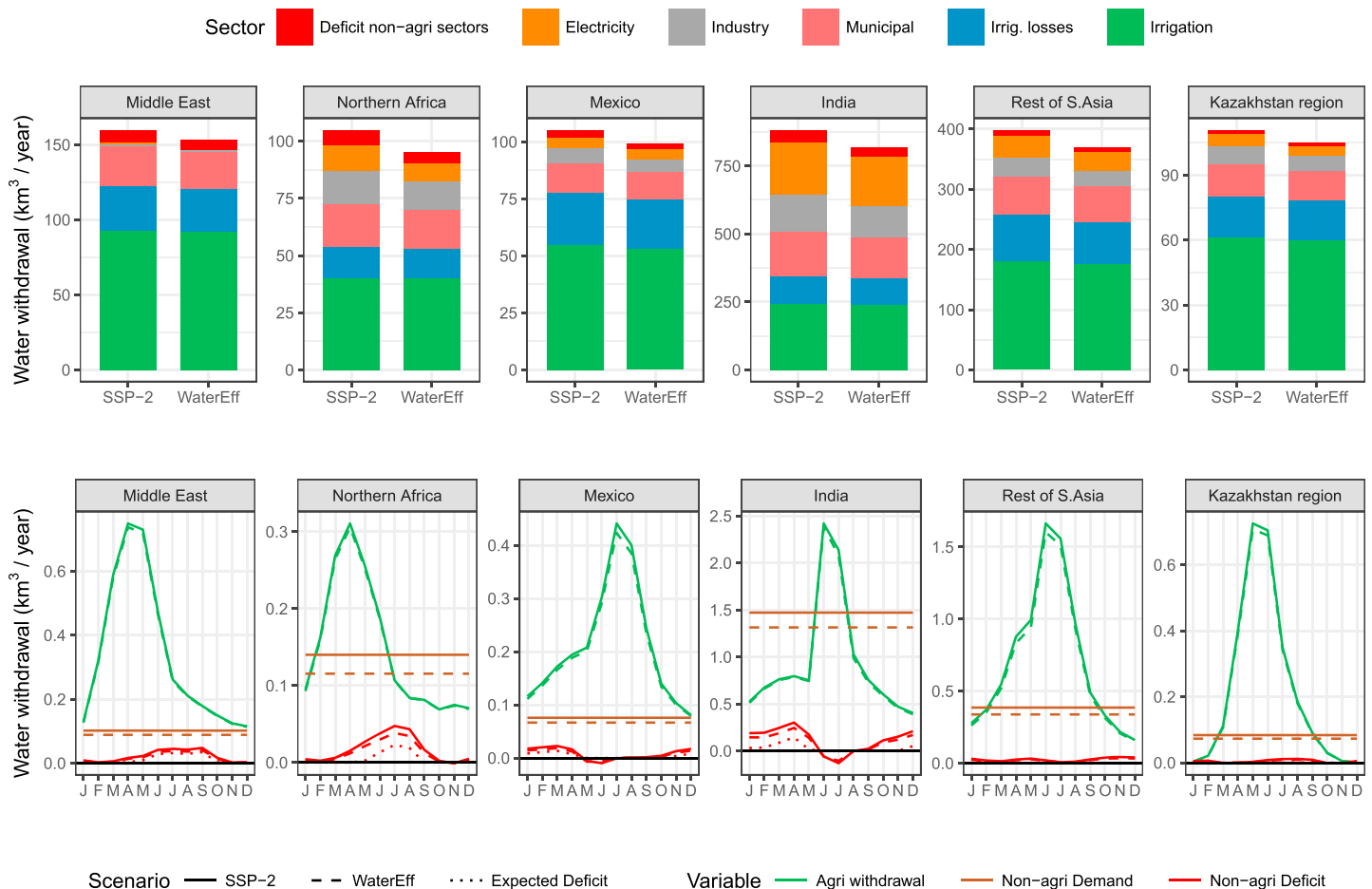
Figure 6. Potential for resource efficiency improvements to reduce water demand and nonagricultural water deficits (WaterEff compared to SSP-2), based on average flows in 2048–2052. Only regions are shown for which withdrawal deficit >5% of nonagricultural demand (top row). In the bottom row, expected deficit (red dotted line) indicates what the remaining deficit would be if the SSP-2 deficit (red solid line) were reduced by the same amount (km^3/yr) as the demand reduction (difference between brown solid and dashed lines).

average peak of only 13%, whereas it is 27% versus 23% in Russia. For India and Turkey, most of the interannual variation takes place in months with high water deficits. The highest peak deficit for India is 32% versus 20% on average, and for Turkey it is 23% versus 14% on average.

The right-hand side in Figure 5 displays the net annual deficit for each year, taking into account the compensating effect of "negative deficits" when local water storage is replenished. For India and Turkey, the high peak water deficit in a specific year is partly compensated by higher replenishment in subsequent months, resulting in only slightly higher net annual deficits. By contrast, there are other regions for which deficits are higher throughout the year for some years, resulting in higher interannual variability of net annual deficits. This seems to happen in Mexico, rest of Southern Asia, South Africa, rest of Southern Africa, rest of Southern America, and Oceania.

3.4. Effects of Increased Efficiency

Studies have indicated that there is ample room to improve water use efficiencies. Therefore, we estimate the potential for efficiency improvements to reduce water demand and water deficits, by applying the higher water use efficiencies from SSP-1 to the SSP-2 scenario (see section 2.2). The impact on allocated water withdrawal and deficit in 2050 for the most deficit-prone regions is shown in Figure 6.

Figure 6 (top row) shows that water use efficiency improvements in the electricity, industry, and municipal sector could significantly reduce nonagricultural water demand in 2050 in the Middle East (13%), Northern

Africa (18%), Mexico (12%), India (11%), rest of Southern Asia (12%), and Kazakhstan region (13%). Additionally, irrigation efficiency improvements reduce irrigation water use between 1.4% (Northern Africa) and 4.2% (rest of Southern Asia). The overall reductions in demand are large enough to almost eliminate water deficits at the annual, regional level in 2050: 7 km^3/yr demand reduction versus 8 km^3/yr deficit in the Middle East, 10 versus 6 km^3/yr in Northern Africa, etc. However, significant water deficits remain in all regions under the WaterEff scenario: 7 km^3/yr (or 21% of nonagricultural demand) in the Middle East, 5 km^3/yr or 12% in Northern Africa, 2 km^3/yr or 9% in Mexico, 33 km^3/yr or 7% in India, 8 km^3/yr or 6% in rest of Southern Asia, and 1 km^3/yr or 5% in Kazakhstan region. Since the aggregate demand reductions in WaterEff are larger than the deficits in SSP-2, one would expect the deficits to disappear in WaterEff. Therefore, the significant deficits that remain must be the result of spatial and/or temporal mismatches between supply and demand. This highlights the importance of our detailed modeling approach.

The bottom row of Figure 6 shows the seasonal patterns for nonagricultural demand, water allocated to agriculture, and the water withdrawal deficit for nonagricultural sectors. In the WaterEff scenario (dashed lines), nonagricultural demand and deficits are somewhat lower compared to SSP-2 (solid lines). For Northern Africa, it can be clearly seen that the deficit reduction (difference between solid and dashed red lines) is largest at the peak of deficit, in July. However, the deficit reduction in any month is smaller than the demand reduction (difference between solid and dashed brown lines). If there would be no spatial structure or heterogeneity within the region, one would expect the demand reduction (km^3) to result in an equal reduction of the deficit. This "expected deficit" is indicated by the red dotted line in Figure 6, but the actual deficit in the WaterEff scenario is higher (red dashed lines). The area under the red dots is the WaterEff deficit mostly due to seasonality, and the area between the red dotted and red dashed lines is the deficit due to spatial mismatch between water demand and availability.

3.5. Effects of Allocation Mechanisms

When water is scarce, the effects of different mechanisms for allocating the water become important. In Figure 7, we contrast the results above (OtherFirst) with an allocation rule where irrigation gets priority (IrrigFirst) and one in which the irrigated land area does not change after 2005 (IrrigConst). The latter scenario simulates the possibility that nonagricultural sectors use their economic and/or political power to prevent further expansion of irrigated lands.

Figure 7 shows the effects of different allocation mechanisms on water deficit for the nonagricultural sectors. The water deficit shown here is the net amount at the annual level (sum of the monthly deficits and the storage replenishment/postponed demand fulfillment after a period of shortage; see section 2.1.3). Relative to demand (left panel), the largest deficits by far are projected for the Middle East, but per capita (center panel) the deficits can be equally large in Northern Africa, Mexico, India, rest of Southern Asia, the Kazakhstan region, and Russia.

The priority order has a clear effect on deficits. The center panel shows that nonagricultural deficits in absolute terms are clearly much lower in the scenario in which nonagricultural water uses are prioritized (OtherFirst) than the scenario in which irrigation is prioritized (IrrigFirst): 47% lower in the Middle East, 28% in Northern Africa, 32% in Mexico, 48% in India, 55% in rest of Southern Asia, 70% in Turkey, and 38% in Kazakhstan region. The difference between the two scenarios also indicates how much irrigation and other sectors compete directly at the local level, since this is the impact of reversing the priority rules at the grid cell level and daily time step.

The panel on the right in Figure 7 shows the withdrawal volume allocated to irrigation use, in m^3/capita/year. The scenario without expansion of irrigated land (IrrigConst) results in 8–22% less water withdrawal compared to OtherFirst in the Middle East, Northern Africa, Mexico, Turkey, Kazakhstan region, rest of South America, and China. However, the reduction of irrigation has virtually no effect on annual deficits for the nonagricultural sectors (left and center panels).

4. Discussion

4.1. All Scenarios in Perspective

In section 3 we have compared future scenarios, focusing on socioeconomic drivers (section 3.2), efficiency gains (section 3.4), and allocation priority rules (section 3.5). Here we compare all scenarios at once, in
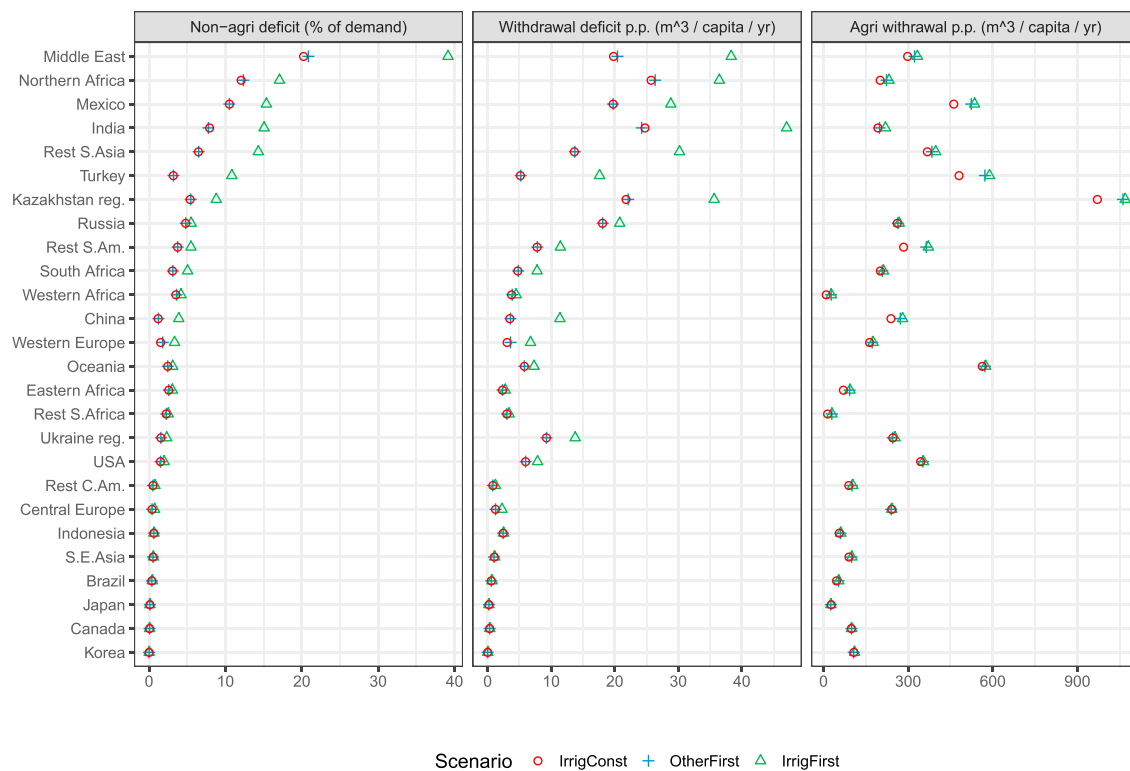
Figure 7. Nonagricultural water deficit relative to demand (left) and per capita (center), and irrigation water withdrawal per capita (right) in SSP-2, 2048–2052, under various allocation mechanisms. Regions are sorted by relative water deficit for the nonagricultural sectors.

order to show the relative magnitudes of their effects on allocated irrigation water, nonagricultural water demand, and annual withdrawal deficit for the nonagricultural sectors (Figure 8).

The top row of Figure 8 shows that the volume of water allocated to irrigation is different for each scenario, but the distribution over the regions is roughly the same. Compared to 2010, in 2050 global total irrigation projected to increase by 15% in SSP-3, 10% in IrrigFirst, 6% in SSP-2, and 3% in WaterEff, whereas it is projected to decrease by 2% in SSP-1 and 4% in IrrigConst due to faster irrigation efficiency improvements in developing regions. The relatively slow growth in water demand for irrigation is consistent with literature (Elliott et al., 2014; Wada et al., 2013).

The second row in Figure 8 shows that from 2010 to 2050, nonagricultural water withdrawal demand increases under all scenarios, by at least 33% (in SSP-1) and up to 55% (in SSP-2) at the global level. A comparison of three different models showed for SSP2 a range of 25–125% increase, with an average of 85% (Wada et al., 2016), showing that our results are within this range—although on the low side (in an earlier paper, we discussed that the main reason is that we assume a higher efficiency increase; Bijl et al., 2016). Regional patterns across the models are comparable showing most increase in Africa and Asia (Satoh et al., 2017; Wada et al., 2016). In the WaterEff scenario, the socioeconomic drivers from SSP-2 combined with the efficiencies of SSP-1 result in a nonagricultural demand increase of 37% during 2010–2050. Compared to SSP-2, nonagricultural demand in WaterEff in 2050 is 12% lower globally and 9–24% lower at the regional level. Nonagricultural demand in IrrigFirst and IrrigConst is equal to SSP-2 by definition.

Water deficits (bottom row of Figure 8) also increase for all scenarios over the period 2010–2050, ranging from a factor 2.1 (WaterEff) to 4.8 (IrrigFirst). The major regions with deficits in 2050 are India, rest of Southern Asia, the Middle East, Northern Africa, and China, which together make up about three quarters of global deficit in all scenarios (see, for instance, also Liu et al., 2017; Schewe et al., 2014). Compared to SSP-2, extra water efficiency in the WaterEff scenario reduces nonagricultural deficit by 21% at the global level and by 12–33% in the regions. The IrrigFirst scenario shows that the priority rules governing water allocation at the local level have a large effect on overall deficit: 45% lower in OtherFirst (SSP-2) compared to IrrigFirst globally and up to 80% lower at the regional level.
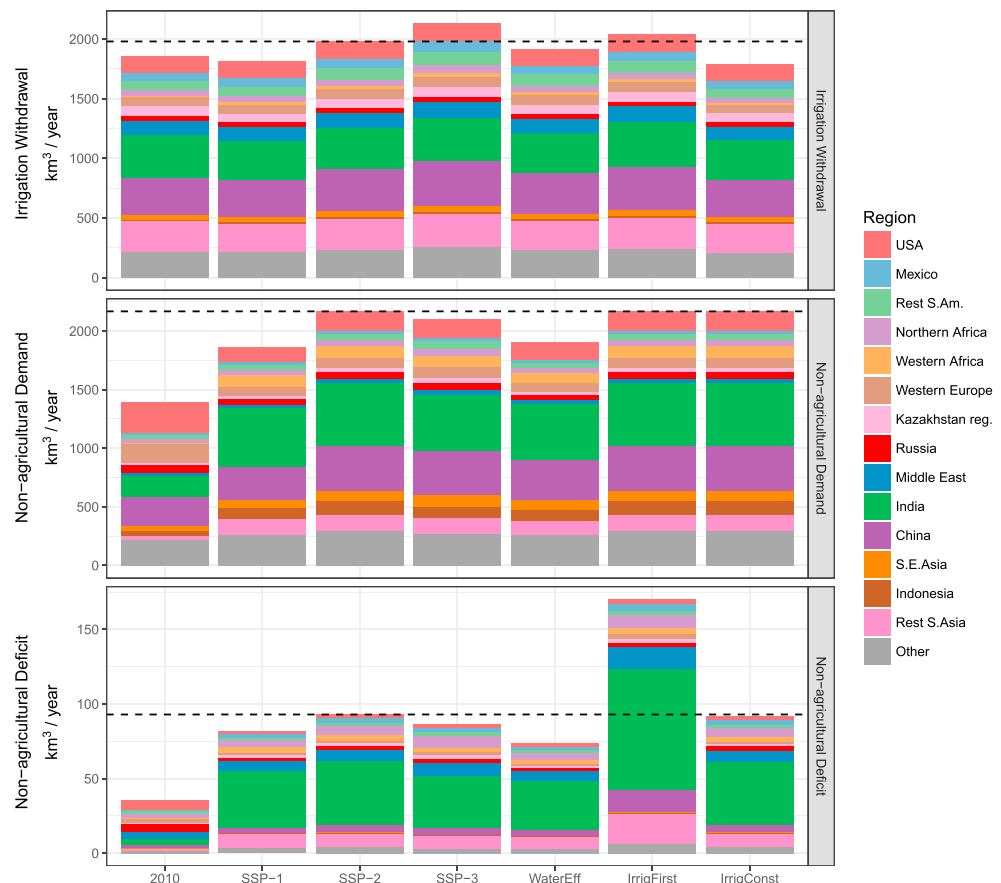
Figure 8. Comparing withdrawal demands and deficit (rows) for 2050, for all regions (colors) and scenarios (columns), using 2010 as reference (first column). The dotted line indicates the level in SSP-2 in 2050.

4.2. Comparison to Other Studies and Suggestions for Further Research

The IMAGE-LPJmL model represents a current state-of-the-art IAM of water supply and demand, in terms of both detail and breadth of processes covered. For this paper we decided to use RCP climate projections that are roughly consistent with the three SSPs (RCP 3.4 for SSP-1 and 4.5 for all other scenarios). This setup does not include direct feedbacks from the emissions to the climate. However, the setup has the advantage that SSP-3, SSP-2, and the variants of SSP-2 can be directly compared due to the same climates. Based on our analyses, we found that the representation of relevant supply and demand dynamics at the grid level can be improved.

Although water availability is simulated in great detail, including irrigation water use and surface water availability, the simulated remaining demand might still be met in reality by other processes. We found large intra-annual and interannual variations in water deficit for different regions. These variations might be partly buffered by abstraction of groundwater (Döll et al., 2014; Wada et al., 2014b), which can in theory buffer these extremes. A further step in development of the SSPs is also to include technological solutions to increase water availability at the grid cell, for example, the contribution of long-distance canals and desalination (Hanasaki et al., 2018).

Regarding the seasonal or monthly patterns in water scarcity, the findings in section 3.2 are broadly consistent with previous studies, which are based on different models (Hanasaki et al., 2008; Hoekstra et al., 2012; Wada et al., 2011). In all cases, the Middle East, Northern Africa, India, and Mexico are highlighted as areas with the largest seasonal variation of water stress or deficit. However, a direct and more detailed comparison is difficult since the metric used for water scarcity differs. For the MENA (Middle East and North Africa) region, Droogers et al. (2012) already showed an enormous shortage in water availability over the coming years, with an increase in unmet demand by 370% in 2050. Although the increase in water shortage is largely caused by

increases in demand, De Wit and Stankiewicz (2006) show, for instance, that the estimated climate change will lead to a decrease in perennial drainage, resulting in a significant decrease of 25% regarding access to surface water across Africa in 2100.

One of the innovations in our model is that allocation is based on withdrawal (the allocated consumption for the nonagricultural sectors is reduced proportionally in case of deficits). The main benefit of this approach is that electricity generation using once-through cooling (high withdrawal and low consumption) encounters limitations due to water availability much earlier, that is, is more realistic. The model could be improved further by taking into account the current and likely future locations of specific types of power plants. Also, improvements can be found by a better representation of the exact geographical location of water withdrawal from the groundwater and transport via, for instance, aquaduct systems, as done by Hanasaki et al. (2018). Various other improvements are possible in the methods for downscaling and modeling seasonal effects. For example, the effects of urbanization in the future have not yet been included in the model (e.g., Chen et al., 2014). Changing habitation patterns over time would make the long-term simulation more realistic but would also introduce yet another explanatory variable and source of uncertainty. Another point is that the current downscaling method does not utilize average yearly temperature, whereas a city with a hot local climate would use a larger fraction of the regional total as compared to a similarly sized city in a cold location (e.g., Zakšek & Oštir, 2012). Since the temperature in the grid cells also depends on the season, temperature-based seasonality could also be introduced to the nonagricultural water demand. However, the sensitivity to temperature will differ per sector and the consumption-withdrawal ratio would probably change as well. Likewise, the method could also use the monthly information on the use of power plants, including peak electricity demand and renewable electricity production.

In this version of the model, local water scarcity does not dynamically influence water efficiency factors in electricity, industry, and municipal sectors. Future model improvements could include these dynamic effects, so that water-scarce grid cells implement efficiency improvements faster than water-abundant cells, which would also make the regional average efficiency improvements endogenous instead of exogenous (see also Neverre et al., 2016).

The current study focused on water allocation for human use only. Any application of this or other water allocation scheme should include nonhuman use as well. For this purpose, one of the many environmental flow frameworks could be applied. Complexity of these frameworks ranges from very simplistic hydrology-based approaches, where only a defined minimum flow is required, toward more holistic approaches where the interaction between streamflow and ecosystem functioning is considered (Poff et al., 2017; Tharme, 2003). One particular challenge here is to strike a balance between method sophistication and data availability, especially on the global scale.

Although even the most optimistic scenario in Figure 8 projects global water deficit to double over the period 2010–2050, this is by no means certain. First of all, there might be more room for increased efficiency than considered here. Other strategies for avoiding future water deficits, not considered here, include (1) recycling water more often between sectors in the same location (e.g., from electricity generation, to municipal and industrial uses, then to local irrigation); (2) building additional water storage reservoirs (also in flat terrain) and artificial groundwater recharge using natural aquifers; (3) encouraging agriculture, industry, and even population to relocate to more water-abundant locations; and (4) optimizing water use at the basin level (see also Gleick, 2003; Wada et al., 2014a). These have not yet been implemented in the model, partly because the applicability of these solution strategies depends on additional data at the local level, with global coverage. The fourth strategy, basin-level optimization, is complex for modeling since it needs to take into account local hydrological factors such as flow direction and spatially heterogeneous demand, as well as a basin-level strategy. For example, basin-level optimization could include that for any particular water-scarce location (e.g., a large city), the whole upstream catchment is analyzed to find locations where water is consumed with the least added value, and then users in those locations are paid to forego that water consumption (e.g., by buying irrigation rights). Our scenario IrrigConst is only a first exploration of the impact of such a strategy.

In our paper we have shown that competition dynamics in the grid cell are highly important. As food and water security are inextricably intertwined, it means that socioeconomic and environmental changes in one part of the globe have cascading effects throughout due to the highly complex trade systems (see also D'Odorico et al., 2010). Further, these cross-scale feedbacks are having impacts on all sectors. In a next step, to

account for competition dynamics in the water-food-energy nexus, alternative approaches should be developed, as the multiagent network of city agents developed by Dermody et al. (2017), which are connected to the infrastructural trade network.

5. Conclusion

In the absence of specific new policies to respond to water scarcity, global water withdrawal is projected to increase significantly for all SSP scenarios over the period 2010–2050, driven mostly by the municipal and electricity sectors and with rapid increases in some regions. Total water withdrawal is projected to increase by 12% in SSP-1, 26% in SSP-2, and 29% in SSP-3, despite the assumed efficiency improvements in each scenario. All scenarios show increasing water withdrawal in the municipal sector: 311–366 additional km^3/yr. Water withdrawal for electricity generation increases in SSP-2 (+221 km^3/yr) and SSP-3 (+303 km^3/yr). Irrigation water withdrawal increases mainly in SSP-3 (+270 km^3/yr including conveyance losses). For some regions, all three SSPs result in rapidly increasing water withdrawal: India (about 1% per annum), Indonesia and Eastern Africa (almost 2% p.a.), rest of Southern Africa (3.5% p.a.), and Western Africa (4% p.a.).

Water deficits for the nonagricultural sectors are small in 2010 but become significant in the future, specifically in India and Southern Asia, Mexico, the Middle East, and Northern Africa, and especially in terms of seasonal patterns. At the annual level, water deficits in 2048–2052 under SSP-2 are 21% of nonagricultural demand in the Middle East and 7–12% in Northern Africa, Mexico, India, and rest of Southern Asia. Seasonal deficits (average of 2045–2055) are highest in the Middle East and Northern Africa, where peak monthly water deficit surpasses 40% and 30% of demand, respectively, while deficits last for many consecutive months. The water supply in even the most water-abundant months is not enough to replenish short-term water storage and thus compensate for some of the deficits. In India, rest of Southern Asia, and Mexico, water deficits increase in the autumn and winter but are partly compensated when plenty of water becomes available in May, June, and July. In Russia and the Ukraine region, water deficits have a much shorter duration but still reach a peak in December of 23% and 13%, respectively. Overall, the deficit in each region is a clear indicator of water scarcity, although unmet demand might still be met by using groundwater, long-distance canals, desalination, long-term storage, or improved water management at the watershed scale.

Interannual variability of precipitation is reflected in interannual variability of future water deficits. Although the seasonal pattern of water deficits is fairly consistent in Northern Africa and the Middle East, the risk of negative surprises is higher in Mexico, India, Turkey, and the Ukraine region. Within a sample of 11 years, 2045–2055, the peak monthly deficit reaches 47% for Mexico, whereas the average seasonal pattern reaches 29% deficit. Similar variability in deficits is shown for India, Turkey, and the Ukraine region. However, in terms of net annual deficit, the interannual variability is high for Mexico (again), rest of Southern Asia, South Africa, rest of Southern Africa, rest of Southern America, and Oceania.

Extra water use efficiency improvements, along the lines of SSP-1 rather than SSP-2, could significantly reduce water withdrawal in 2050 but have less impact on water deficits. Compared to SSP-2, faster improvements in nonagricultural water use efficiency could result in significantly lower demand in 2050, in water-scarce regions: 11–18% lower in the Middle East, Northern Africa, Mexico, India, rest of Southern Asia, and Kazakhstan region. Increased irrigation efficiency also saves 1.4–4.2% on irrigation withdrawal in these regions. However, the water savings in km^3 do not result in an equal volume-wise reduction of water deficits for the nonagricultural sectors. Although the volume of water saved is enough to more or less eliminate the water deficits, the deficits are reduced by only 16–22% in these regions, 21% at the global level, and up to 33% in other regions. Thus, in these water-scarce regions more than 78% of the deficits remain, and the deficit relative to demand remains roughly unchanged (5–21%). This indicates a fundamental spatial and/or temporal mismatch between water availability and demand within these regions and highlights the importance of our detailed modeling approach using grid cells.

Different priority rules at the local level have a large impact on nonagricultural water deficits, whereas limiting the expansion of irrigated land has very little effect. Global nonagricultural water deficit around 2050 is 45% lower when nonagricultural sectors are prioritized over irrigation at the local level (OtherFirst scenario) compared to the reverse (IrrigFirst), and the difference is 28–70% for the regions with the largest deficits. Conversely, the scenario without expansion of irrigated land (IrrigConst) has virtually no effect on annual

deficits, even though irrigation receives 8–22% less water in the Middle East, Northern Africa, Mexico, Turkey, Kazakhstan region, rest of South America, and China.

This paper represents a new step in the integrated modeling of complex economic and hydrological processes at a global scale. Whereas previous efforts were still clearly slanted toward either economics (missing local hydrology) or hydrology (missing economic feedbacks), our use of the coupled IMAGE-LPJmL model includes both worlds more fully. In particular, we simulated intersectoral water allocation rules at the 0.5° × 0.5° grid scale with a daily time step and include both withdrawal and consumption in this process. Further research is needed to improve the model even further, for instance, by taking into account the likely locations of specific types of power plants, by including seasonality and local temperature in nonagricultural water demand, and by implementing strategies for coping with water deficits such as local efficiency improvement, local recycling water between sectors, and letting downstream users influence their upstream catchment.

References

Alcamo, J., Döll, P., Henrichs, T., Kaspar, F., Lehner, B., Rösch, T., & Siebert, S. (2003). Development and testing of the WaterGAP 2 global model of water use and availability. *Hydrological Sciences Journal*, *48*(3), 317–337. https://doi.org/10.1623/hysj.48.3.317.45290

Amarasinghe, U. A., & Smakhtin, V. (2014). Global water demand projections: Past, present and future. International Water Management Institute (IWMI).

Arnell, N. W., Van Vuuren, D. P., & Isaac, M. (2011). The implications of climate policy for the impacts of climate change on global water resources. *Global Environmental Change*, *21*(2), 592–603. https://doi.org/10.1016/j.gloenvcha.2011.01.015

Biemans, H., Haddeland, I., Kabat, P., Ludwig, F., Hutjes, R. W. A., Heinke, J., et al. (2011). Impact of reservoirs on river discharge and irrigation water supply during the 20th century. *Water Resources Research*, *47*, W03509. https://doi.org/10.1029/2009WR008929

Bijl, D. L., Bogaart, P. W., Kram, T., De Vries, B. J. M., & Van Vuuren, D. P. (2016). Long-term water demand for electricity, industry and households. *Environmental Science & Policy*, *55*, 75–86. https://doi.org/10.1016/j.envsci.2015.09.005

Bondeau, A., Smith, P. C., Zaehle, S., Schaphoff, S., Lucht, W., Cramer, W., et al. (2007). Modelling the role of agriculture for the 20th century global terrestrial carbon balance. *Global Change Biology*, *13*(3), 679–706. https://doi.org/10.1111/j.1365-2486.2006.01305.x

Bos, M. G., & Wolters, W. (1990). Water charges and irrigation efficiencies. *Irrigation and Drainage Systems*, *4*(3), 267–278. https://doi.org/10.1007/BF01117746

Chen, M., Zhang, H., Liu, W., & Zhang, W. (2014). The global pattern of urbanization and economic growth: Evidence from the last three decades. *PLoS One*, *9*(8), e103799. https://doi.org/10.1371/journal.pone.0103799

Climatic Research Unit (2017). Climatic Research Unit Data [WWW Document]. Retrieved from http://www.cru.uea.ac.uk/data (accessed 6.6.17).

Dalin, C., Wada, Y., Kastner, T., & Puma, M. J. (2017). Groundwater depletion embedded in international food trade. *Nature*, *543*(7647), 700–704. https://doi.org/10.1038/nature21403

De Wit, M., & Stankiewicz, J. (2006). Changes in surface water supply across Africa with predicted climate change. *Science*, *311*(5769), 1,917–1,921. https://doi.org/10.1126/science.1119929

Dellink, R., Chateau, J., Lanzi, E., & Magné, B. (2017). Long-term economic growth projections in the shared socioeconomic pathways. *Global Environmental Change*, *42*, 200–214. https://doi.org/10.1016/j.gloenvcha.2015.06.004

Dermody, B. J., Sivapalan, M., Stehfest, E., van Vuuren, D. P., Wassen, M. J., Bierkens, M. F. P., & Dekker, S. C. (2017). A framework for modelling the complexities of food and water security under globalisation. *Earth System Dynamics Discussions*, 1–27. https://doi.org/10.5194/esd-2017-38

D'Odorico, P., Laio, F., & Ridolfi, L. (2010). Does globalization of water reduce societal resilience to drought?: Water globalization and resilience. *Geophysical Research Letters*, *37*, L10403. https://doi.org/10.1029/2010GL043167

Doelman, J. C., Stehfest, E., Tabeau, A., van Meijl, H., Lassaletta, L., Gernaat, D. E. H. J., et al. (2018). Exploring SSP land-use dynamics using the IMAGE model: Regional and gridded scenarios of land-use change and land-based climate change mitigation. *Global Environmental Change*, *48*, 119–135. https://doi.org/10.1016/j.gloenvcha.2017.11.014

Döll, P., Müller Schmied, H., Schuh, C., Portmann, F. T., & Eicker, A. (2014). Global-scale assessment of groundwater depletion and related groundwater abstractions: Combining hydrological modeling with information from well observations and GRACE satellites. *Water Resources Research*, *50*, 5,698–5,720. https://doi.org/10.1002/2014WR015595

Droogers, P., Immerzeel, W. W., Terink, W., Hoogeveen, J., Bierkens, M. F. P., van Beek, L. P. H., & Negewo, B. D. (2012). Modeling water resources trends in Middle East and North Africa towards 2050. *Hydrology and Earth System Sciences Discussions*, *9*(4), 4,381–4,416. https://doi.org/10.5194/hessd-9-4381-2012

Elliott, J., Deryng, D., Müller, C., Frieler, K., Konzmann, M., Gerten, D., et al. (2014). Constraints and potentials of future irrigation water availability on agricultural production under climate change. *Proceedings of the National Academy of Sciences*, *111*(9), 3,239–3,244. https://doi.org/10.1073/pnas.1222474110

FAOSTAT (2016). FAO statistical databases [WWW Document]. URLhttp://faostat3.fao.org/home/index.html (accessed 2.3.16).

Fujimori, S., Hanasaki, N., & Masui, T. (2016). Projections of industrial water withdrawal under shared socioeconomic pathways and climate mitigation scenarios. *Sustainability Science*, https://doi.org/10.1007/s11625-016-0392-2, *12*(2), 275–292

Gerten, D., Heinke, J., Hoff, H., Biemans, H., Fader, M., & Waha, K. (2011). Global water availability and requirements for future food production. *Journal of Hydrometeorology*, *12*(5), 885–899. https://doi.org/10.1175/2011JHM1328.1

Gleeson, T., Wada, Y., Bierkens, M. F. P., & Van Beek, L. P. H. (2012). Water balance of global aquifers revealed by groundwater footprint. *Nature*, *488*(7410), 197–200. https://doi.org/10.1038/nature11295

Gleick, P. H. (2003). Global freshwater resources—Soft-path solutions for the 21st century. *Science*, *302*(5650), 1,524–1,528. https://doi.org/10.1126/science.1089967

Gosling, S. N., & Arnell, N. W. (2016). A global assessment of the impact of climate change on water scarcity. *Climatic Change*, *134*(3), 371–385. https://doi.org/10.1007/s10584-013-0853-x

Haddeland, I., Skaugen, T., & Lettenmaier, D. P. (2006). Anthropogenic impacts on continental surface water fluxes. *Geophysical Research Letters*, *33*, L08406. https://doi.org/10.1029/2006GL026047

Hanasaki, N., Fujimori, S., Yamamoto, T., Yoshikawa, S., Masaki, Y., Hijioka, Y., et al. (2013). A global water scarcity assessment under Shared Socio-Economic Pathways. Part 1: Water use. *Hydrology and Earth System Sciences*, *17*(7), 2375–2391. https://doi.org/10.5194/hess-17-2375-2013

Hanasaki, N., Kanae, S., & Oki, T. (2006). A reservoir operation scheme for global river routing models. *Journal of Hydrology*, *327*(1-2), 22–41. https://doi.org/10.1016/j.jhydrol.2005.11.011

Hanasaki, N., Kanae, S., Oki, T., Masuda, K., Motoya, K., Shirakawa, N., et al. (2008). An integrated model for the assessment of global water resources–part 2: Applications and assessments. *Hydrology and Earth System Sciences*, *12*(4), 1,027–1,037. https://doi.org/10.5194/hess-12-1027-2008

Hanasaki, N., Yoshikawa, S., Pokhrel, Y., & Kanae, S. (2018). A global hydrological simulation to specify the sources of water used by humans. *Hydrology and Earth System Sciences*, *22*, 789–817. https://doi.org/10.5194/hess-22-789-2018

Hejazi, M., Edmonds, J., Clarke, L., Kyle, P., Davies, E., Chaturvedi, V., et al. (2014). Long-term global water projections using six socioeconomic scenarios in an integrated assessment modeling framework. *Technological Forecasting and Social Change*, *81*, 205–226. https://doi.org/10.1016/j.techfore.2013.05.006

Hoekstra, A. Y., Mekonnen, M. M., Chapagain, A. K., Mathews, R. E., & Richter, B. D. (2012). Global monthly water scarcity: Blue water footprints versus blue water availability. *PLoS One*, *7*(2), e32688. https://doi.org/10.1371/journal.pone.0032688

IPCC-DDC (2007). AR4 GCM data: SRES scenarios. [WWW Document]. Retrieved from http://www.ipcc-data.org/sim/gcm_monthly/SRES_AR4/index.html

Johansson, R. C., Tsur, Y., Roe, T. L., Doukkali, R., & Dinar, A. (2002). Pricing irrigation water: A review of theory and practice. *Water Policy*, *4*(2), 173–199. https://doi.org/10.1016/S1366-7017(02)00026-0

K. C., S., & Lutz, W. (2017). The human core of the shared socioeconomic pathways: Population scenarios by age, sex and level of education for all countries to 2100. *Global Environmental Change*, *42*, 181–192. https://doi.org/10.1016/j.gloenvcha.2014.06.004

Kim, S. H., Hejazi, M., Liu, L., Calvin, K., Clarke, L., Edmonds, J., et al. (2016). Balancing global water availability and use at basin scale in an integrated assessment model. *Climatic Change*, *136*(2), 217–231. https://doi.org/10.1007/s10584-016-1604-6

Klein Goldewijk, K., Beusen, A., & Janssen, P. (2010). Long-term dynamic modeling of global population and built-up area in a spatially explicit way: HYDE 3.1. *The Holocene*, *20*(4), 565–573. https://doi.org/10.1177/0959683609356587

Lehner, B., Liermann, C. R., Revenga, C., Vörösmarty, C., Fekete, B., Crouzet, P., et al. (2011). High-resolution mapping of the world's reservoirs and dams for sustainable river-flow management. *Frontiers in Ecology and the Environment*, *9*(9), 494–502. https://doi.org/10.1890/100125

Liu, J., Yang, H., Gosling, S. N., Kummu, M., Flörke, M., Pfister, S., et al. (2017). Water scarcity assessments in the past, present, and future: Review on water scarcity assessment. *Earths Future*, *5*(6), 545–559. https://doi.org/10.1002/2016EF000518

Mayer, P. W., DeOreo, W. B., Opitz, E. M., Kiefer, J. C., Davis, W. Y., Dziegielewski, B., & Nelson, J. O. (1999). Residential end uses of water. AWWA Research Foundation and American Water Works Association Denver, CO.

Meinshausen, M., Raper, S. C. B., & Wigley, T. M. L. (2011). Emulating coupled atmosphere-ocean and carbon cycle models with a simpler model, MAGICC6—Part 1: Model description and calibration. *Atmospheric Chemistry and Physics*, *11*(4), 1417–1456. https://doi.org/10.5194/acp-11-1417-2011

Molle, F., & Berkoff, J. (2009). Cities vs. agriculture—A review of intersectoral water re-allocation. *Natural Resources Forum*, *33*, 6–18.

Neverre, N., Dumas, P., & Nassopoulos, H. (2016). Large-scale water scarcity assessment under global changes: Insights from a hydroeconomic framework. *Hydrology and Earth System Sciences Discussions*, 1–26. https://doi.org/10.5194/hess-2015-502

O'Neill, B. C., Kriegler, E., Ebi, K. L., Kemp-Benedict, E., Riahi, K., Rothman, D. S., et al. (2017). The roads ahead: Narratives for shared socioeconomic pathways describing world futures in the 21st century. *Global Environmental Change*, *42*, 169–180. https://doi.org/10.1016/j.gloenvcha.2015.01.004

O'Neill, B. C., Kriegler, E., Riahi, K., Ebi, K. L., Hallegatte, S., Carter, T. R., et al. (2014). A new scenario framework for climate change research: The concept of shared socioeconomic pathways. *Climatic Change*, *122*(3), 387–400. https://doi.org/10.1007/s10584-013-0905-2

Parkinson, S. C., Johnson, N., Rao, N. D., Jones, B., van Vliet, M. T. H., Fricko, O., et al. (2016). Climate and human development impacts on municipal water demand: A spatially-explicit global modeling framework. *Environmental Modelling and Software*, *85*, 266–278. https://doi.org/10.1016/j.envsoft.2016.08.002

Poff, N. L., Tharme, R. E., & Arthington, A. H. (2017). Evolution of environmental flows assessment science, principles, and methodologies. In *Water for the environment* (pp. 203–236). London, UK: Elsevier. https://doi.org/10.1016/B978-0-12-803907-6.00011-5

Riahi, K., Van Vuuren, D. P., Kriegler, E., Edmonds, J., O'Neill, B. C., Fujimori, S., et al. (2017). The Shared Socioeconomic Pathways and their energy, land use, and greenhouse gas emissions implications: An overview. *Global Environmental Change*, *42*, 153–168. https://doi.org/10.1016/j.gloenvcha.2016.05.009

Rosegrant, M. W., Meijer, S., & Cline, S. A. (2012). International model for policy analysis of agricultural commodities and trade (IMPACT): Model description. Int. food policy res. Inst. Wash. DC 28.

Rost, S., Gerten, D., Bondeau, A., Lucht, W., Rohwer, J., & Schaphoff, S. (2008). Agricultural green and blue water consumption and its influence on the globalwater system: Global water use in agriculture. *Water Resources Research*, *44*, W09405. https://doi.org/10.1029/2007WR006331

Satoh, Y., Kahil, T., Byers, E., Burek, P., Fischer, G., Tramberend, S., et al. (2017). Multi-model and multi-scenario assessments of Asian water futures: The water futures and solutions (WFaS) initiative—Asian water futures: WFS initiative. *Earths Future*, *5*(7), 823–852. https://doi.org/10.1002/2016EF000503

Schewe, J., Heinke, J., Gerten, D., Haddeland, I., Arnell, N. W., Clark, D. B., et al. (2014). Multimodel assessment of water scarcity under climate change. *Proceedings of the National Academy of Sciences*, *111*(9), 3245–3250. https://doi.org/10.1073/pnas.1222460110

Stehfest, E., Van Vuuren, D. P., Kram, T., Bouwman, A., Alkemade, R., Bakkenes, M., et al. (2014). *Integrated assessment of global environmental change with IMAGE 3.0. Model description and policy applications*. The Hague: PBL Netherlands Environmental Assessment Agency.

Tharme, R. E. (2003). A global perspective on environmental flow assessment: Emerging trends in the development and application of environmental flow methodologies for rivers. *River Research and Applications*, *19*(5-6), 397–441. https://doi.org/10.1002/rra.736

Van Vuuren, D. P., Riahi, K., Calvin, K., Dellink, R., Emmerling, J., Fujimori, S., et al. (2017). The Shared Socio-Economic Pathways: Trajectories for human development and global environmental change. *Global Environmental Change*, *42*, 148–152. https://doi.org/10.1016/j.gloenvcha.2016.10.009

Vorosmarty, C. J. (2000). Global water resources: Vulnerability from climate change and population growth. *Science*, *289*(5477), 284–288. https://doi.org/10.1126/science.289.5477.284

Wada, Y., Flörke, M., Hanasaki, N., Eisner, S., Fischer, G., Tramberend, S., et al. (2016). Modeling global water use for the 21st century: The water futures and solutions (WFaS) initiative and its approaches. *Geoscientific Model Development*, *9*(1), 175–222. https://doi.org/10.5194/gmd-9-175-2016

Wada, Y., Gleeson, T., & Esnault, L. (2014a). Wedge approach to water stress. *Nature Geoscience*, *7*(9), 615–617. https://doi.org/10.1038/ngeo2241

Wada, Y., Van Beek, L. P. H., Viviroli, D., Dürr, H. H., Weingartner, R., & Bierkens, M. F. P. (2011). Global monthly water stress: 2. Water demand and severity of water stress. *Water Resources Research*, *47*, W07518. https://doi.org/10.1029/2010WR009792

Wada, Y., Wisser, D., & Bierkens, M. F. P. (2014b). Global modeling of withdrawal, allocation and consumptive use of surface water and groundwater resources. *Earth System Dynamics*, *5*(1), 15–40. https://doi.org/10.5194/esd-5-15-2014

Wada, Y., Wisser, D., Eisner, S., Flörke, M., Gerten, D., Haddeland, I., et al. (2013). Multimodel projections and uncertainties of irrigation water demand under climate change: Irrigation demand under climate change. *Geophysical Research Letters*, *40*, 4626–4632. https://doi.org/10.1002/grl.50686

Woltjer, G. B., Kuiper, M., Kavallari, A., van Meijl, H., Powell, J. P., Rutten, M. M., et al. (2014). The MAGNET model: Module description. LEI Wageningen UR.

Zakšek, K., & Oštir, K. (2012). Downscaling land surface temperature for urban heat island diurnal cycle analysis. *Remote Sensing of Environment*, *117*, 114–124. https://doi.org/10.1016/j.rse.2011.05.027